Extended Abstracts of the 2002 International Conference on Solid State Devices and Materials, Nagoya, 2002, pp. 344-345

G-4-2

Correlation between Fe-Zn inter-diffusion observed by scanning capacitance microscopy and device characteristics of electro-absorption modulators

M. Ogasawara, R. Iga, S. Kondo*, and Y. Kondo

NTT Photonics Laboratories, 3-1 Morinosato Wakamiya, Atsugi, Kanagawa 243-0198, Japan
Tel:+81 46 240 2755, Fax:+81 46 240 4301, E-mail:moga@aecl.ntt.co.jp

1. Introduction

Fe-Zn inter-diffusion is an important issue in InP-based buried heterostructure optical devices that utilize Zn for p doping and Fe for semi-insulating layers [1]. However, a quantitative method of analyzing this phenomenon has not been established. Scanning capacitance microscopy (SCM) has emerged as a promising technique for high-resolution two-dimensional doping profiling of semiconductor devices [2]. In this study, the SCM technique was applied to analyze Zn diffusion into the semi-insulating burying layer of electro-absorption (EA) modulators. We will demonstrate relationships between the Zn diffusion and characteristics of the modulators.

2. Experimental Procedure

Electro-absorption (EA) modulators with different MQW absorption layer and semi-insulating buying layer were fabricated by means of metalorganic vapor phase epitaxy (MOVPE). Sample structures are summarized in Table I. Mesa width is about 2μm. Iron (Fe) and ruthenium (Ru) were the semi-insulating impurities. It has been reported that Ru does not inter-diffuse with Zn [3]. Fe doping concentrations were varied by changing precursor flow rates. The SCM measurements were performed with a Digital Instruments NanoScope D3100. SCM images were acquired with an alternating-current (AC) bias of 0.2V and direct-current (DC) bias voltages ranging from –2.0 to 2.0V. The DC bias voltage applied to the sample and tip was grounded. All samples were cleaved for cross-sectional imaging.

3. Results and Discussion

Zn diffusion region in the SCM images

Figure 1 shows cross-sectional SCM images of an as-cleaved EA modulator (sample 3) obtained at various DC bias voltages. The images obtained at DC bias voltages of 1.5 and 2.0 V clearly show the Zn diffusion region in which the semi-insulating region is converted into p-type due to Zn diffusion. However, the Zn diffusion region was unclear when the DC bias voltage was less than 1.0 or negative.

Figure 2 compares SCM images and scanning electron microscopy (SEM) images after stain etching [4] of samples 3, 4, and 5. The SCM images clearly show that the Zn diffusion region is reduced with decreasing Fe doping concentration. Indeed, *Zn diffusion lengths*, defined as the lateral extent of Zn diffusion region (dC/dV>0), are 0.9, 0.6, and 0.2μm for samples 3, 4, and 5, respectively. This indicates that Fe-Zn inter-diffusion is suppressed by decreasing Fe doping concentration, and that SCM technique is a powerful tool for quantitative analysis of the Zn diffusion. However, for SEM images the Zn diffusion front was not distinguished clearly. Samples 1 and 2 were also analyzed by SCM (not shown). Zn diffusion length for sample 1 was approximately equal to that for sample 3. But Zn diffusion was not observed for sample 2. This is consistent with the fact that Ru does not inter-diffuse with Zn [3].

Zn diffusion and Device characteristics

Figure 3 shows the relationship between applied bias voltage and capacitances for samples 1 and 2. The results for a polyimide-buried EA modulator with the same MQW absorption layer are included for comparison [5]. The capacitance of sample 2 is lower than that of sample 1 over the entire range of bias voltage. The capacitance of Sample 2 is approximately equal to that of the polyimide-buried EA modulator, in which Zn diffusion never occurs. This indicates that the capacitances are reduced by preventing Zn diffusion.

Figure 4 shows the frequency responses of sample 1, 2 and the polyimide-buried EA modulator [5]. The 3-dB bandwidths are 8, 15, and 19 GHz for samples 1 and 2 and for the polyimide-buried EA modulator, respectively. The frequency responses of samples 3, 4, and 5 were also measured. The 3-dB bandwidths are 10, 12, and 14 GHz for samples 3, 4, and 5. Figure 5 summarizes the relationships between the 3-dB bandwidths and the Zn diffusion lengths. The 3-dB bandwidth increases with decreasing Zn diffusion length irrespective of absorption layer. Therefore, in order to achieve high-speed operation of EA modulators, it is important to prevent the diffusion of Zn into the semi-insulating layers.

4. Conclusion

SCM is demonstrated to be a powerful tool for a quantitative analysis of Zn diffusion. A comparison of the device characteristics of EA modulators showed that Zn diffusion into the semi-insulating burying layer results in increased capacitance and reduced 3-dB bandwidth. Therefore, in order to improve the performance of EA modulators, it is important to prevent the Zn diffusion into the semi-insulating layers.

Acknowledgement

The authors thank Drs. H. Iwamura and Y. Hasumi for their encouragement.

References

[1] E. W. A. Young and G. M. Fontijn, Appl. Phys. Lett., **56**, 146 (1990).

* Present address: Niigata University of International and Information Studies, Niigata-shi 950-2252, Japan.

[2] Y. Huang and C. C. Williams, J. Vac. Sci. Technol. **B12**, 369 (1994).

[3] A. Dadger, O. Stenzel, L. Kohne, A. Naser, M. Strassburg, W. Stolz, D. Bimberg and H. Schmann, J. Cryst. Growth **195**, 69 (1998).

[4] D. T. C. Huo and M. F. Yan, J. Electrochem. Soc., **137**, 3270 (1990).

[5] S. Kondo, Y. Noguchi, K. Tsuzuki, M. Yuda, S. Oku, Y. Kondo and H. Takeuchi, Jpn. J. Appl. Phys. **41**, 1171 (2002).

Table I. Sample Structure

Sample No.	1	2	3	4	5
Absorption layer	InGaAlAs/InAlAs -MQW	InGaAlAs/InAlAs -MQW	InGaAsP/InGaAsP -MQW	InGaAsP/InGaAsP -MQW	InGaAsP/InGaAsP -MQW
Burying layer (Fe,Ru flow rate)	Fe-doped InP (100 sccm)	Ru-doped InP (1000 sccm)	Fe-doped InP (100 sccm)	Fe-doped InP (50 sccm)	Fe-doped InP (30 sccm)

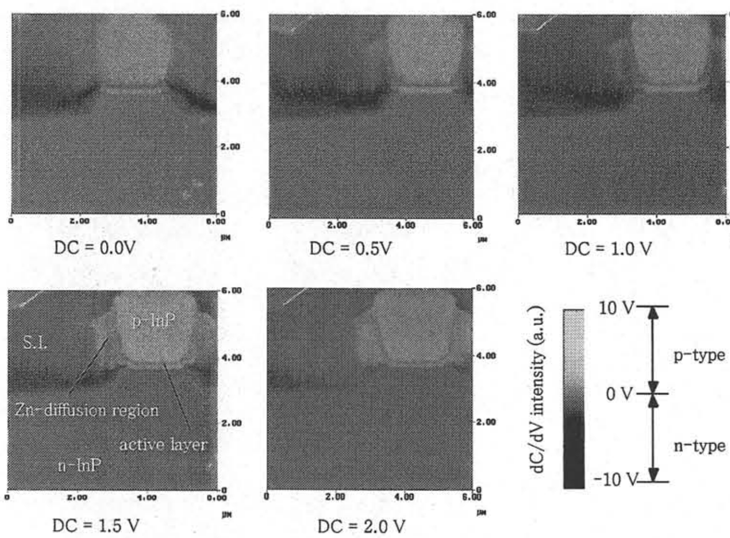

Fig. 1 Cross-sectional SCM images of sample 3.

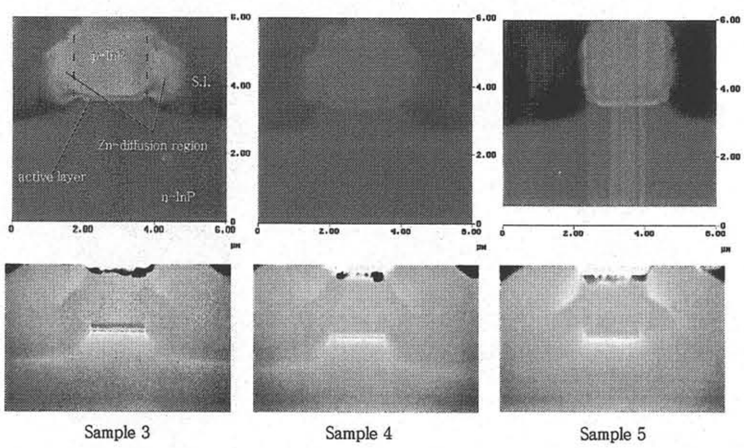

Fig. 2 SCM (upper) and SEM (lower) images of samples 3, 4, and 5.

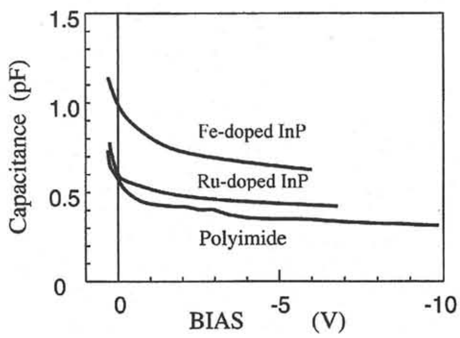

Fig. 3 The capacitance of three modulators.

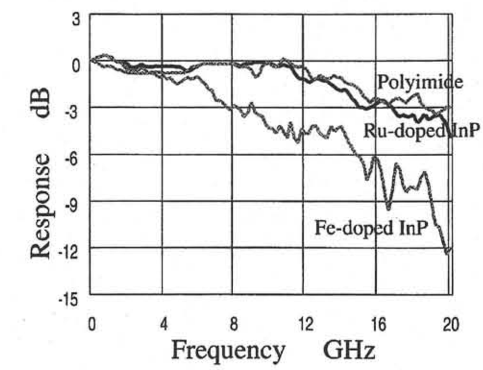

Fig. 4 The frequency response of three modulators.

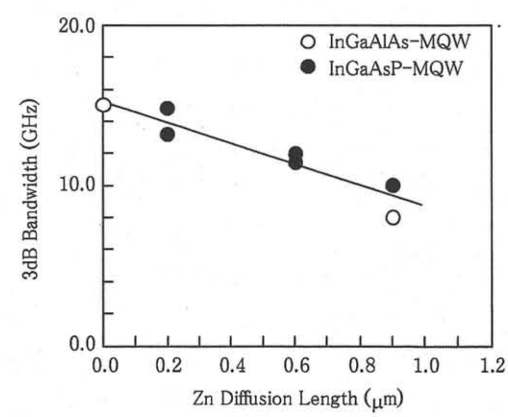

Fig. 5 Dependence of the 3-dB bandwidth and the Zn diffusion length.